RSC Advances

ROYAL SOCIETY OF CHEMISTRY

www.rsc.org/advances

Facile Fabrication of RGO wrapped $LiMn_2O_4$ Nanorods as Cathode with Enhanced Specific Capacity

Jiarui He, Yuanfu Chen*, Pingjian Li*, Fei Fu, Jingbo Liu, and Zegao Wang

State Key Laboratory of Electronic Thin Films and Integrated Devices, University of Electronic Science and Technology of China, Chengdu 610054, P. R. China

* Corresponding authors, E-mail: yfchen@uestc.edu.cn, lipingjian@uestc.edu.cn

Abstract

A facile method with ethanol assisted dispersion combined with magnetic stirrer to prepare reduced graphene oxide (RGO) wrapped $LiMn_2O_4$ nanorods (LNs) is presented. The results show that compared to LNs, LNs/RGO cathode for lithium-ion batteries (LIBs) exhibits much smaller impedance and much better electrochemical performance. After coated RGO, the initial discharge capacity can be increased from 118.9 to 143.5 mAh g^{-1} at 0.2 C which can retain 139.2 mAh g^{-1} after 50 cycles; the rate discharge capacities of LNs/RGO can reach 99.5, 82.1, 56 mAh g^{-1} at 10, 20, 30 C, respectively. The significant performance enhancement can be attributed to the synergetic effect of the $LiMn_2O_4$ nanorods matrix and the conductive graphene wrapping layers. The excellent electrochemical properties make LNs/RGO as promising cathode material for high-performance LIBs. In addition, the facile synthesis routine enables the mass production and can be extended to prepare other graphene wrapped anode or cathode electrodes for LIBs.

Keywords: Graphene, lithium manganese oxide nanorods, cathode

1. Introduction

Rechargeable lithium-ion batteries (LIBs) are key components of both hybrid electric vehicles (HEVs) and full electric vehicles (EVs), requiring high energy and power capability of lithium ion battery.[1-3] Spinel $LiMn_2O_4$ (LMO) is a promising cathode material for applications in HEVs and EVs, owing to its intrinsic low-cost, eco-friendly in nature, abundant manganese resources, and good safety.[4] Therefore, the fast kinetic electrodes are required by the application of LMO in high power systems. Unfortunately, the LMO suffer from low electrical conductivity (~10^{-6} S cm^{-1}) and a tendency of particle agglomeration, which lead to an inferior rate capability.[2]

Many great efforts have been made to increase the electronic conductivity and enhance the rate capability of LMO in recent years.[2] Nanostructured LMO is expected to enhance the rate capability due to the high effective interfacial area between the oxide surface and the electrolyte, and the shorter travel length of lithium ions and electrons during charge/discharge.[6, 7] The other approach is to employ the carbon materials with high electrical conductivity to wrap the LMO to achieve the high rate performance.[8-10] Reduced graphene oxide (RGO) has attracted tremendous attention in electrochemical energy storage due to their large surface area, high electrical conductivity, and good mechanical properties, which are comparable with, or better than, those of carbon nanotubes. Recently, RGO wrapped $LiFePO_4$ or $LiCo_{1/3}Ni_{1/3}Mn_{1/3}O_2$ has been intensively investigated, which exhibit excellent high rate capability and cycling stability.[11-14] Generally, $LiFePO_4$ (LFP) or $LiCo_{1/3}Ni_{1/3}Mn_{1/3}O_2$ (NCM) was firstly wrapped by GO with water as solvent, and then RGO/LFP or RGO/NCM was obtained by annealing at high temperature under argon atmosphere to reduce GO to RGO. It is obvious that such method is very complicated and the crystalline structure and morphology of the cathode or anode might be destroyed during the high temperature reduction process. To avoid the high-temperature reduction process, RGO dry powder can be directly mixed with cathode or anode by ball miller; however, homogeneous RGO wrapped cathode or anode cannot be obtained. Effective RGO wrapping structure can also not be obtained

by mixing RGO powder with cathode or anode in water because RGO cannot be well dispersed in water.

In order to solve such issue mentioned above, herein we present a facile, and environmentally friendly method to directly wrap the $LiMn_2O_4$ nanorods (LNs) cathode by RGO instead of GO with ethanol assisted dispersion combined with magnetic stirrer at ambient temperature in the air. This method can not only avoid the complicated high-temperature reduction process but also keep the high crystallinity and unique morphological properties of LNs. In addition, the present method is environment friendly because the ethanol can be recycled and reused by using rotary evaporator. Most importantly, after wrapped by RGO using this method, LNs/RGO cathode shows smaller impedance, better cycling stability, much higher specific capacity, and much better high-rate performance.

2. Experimental

2.1 Synthesis of RGO

The graphene oxide (GO) was produced from natural graphite by the modified Hummers method, similar to previous report.[15] Thermal exfoliation of as prepared GO was achieved by placing GO in a ceramic boat in a quartz tube furnace at 600 ^oC for 2 h in a gas of Ar with a total flow rate of 150 mL min^{-1} and a heating rate of 5 ^oC min^{-1}.

2.2 Synthesis of β-MnO_2 and LNs

Typically 24 mmol of $MnSO_4 \cdot H_2O$ and 24 mmol of $(NH_4)_2S_2O_8$ were dissolved in 30 mL of deionized water separately to form clear solutions. They were mixed together and transferred to a 100 mL Teflon-lined stainless steel vessel. The vessel was sealed and heated at 150°C for 12 h to obtain β-MnO_2 nanorods. And then, as-synthesized MnO_2 nanorods were mixed and ground with lithium hydroxide (Sigma Aldrich) with a molar ratio of 2:1. A total of 1 mL of methanol was added to make a uniform slurry mixture. The mixture was sintered at 700°C for 10 h under air.[16]

2.3 Synthesis of LNs /RGO

A typical synthesis of RGO-wrapped (LNs) composite was as follows: 50 mg of graphene was dispersed in 25 mL ethanol and ultrasonicated for 2 h, and then 950 mg LNs powder was added to the suspension with magnetic stirrer. And then, the mixture was transfer to the rotary evaporators to dry the mixture and recycle the ethanol at 60°C for several hours. Finally, the as-obtained mixture was dried overnight at 90°C. The mass percentage of graphene is 5 wt %. The Fig. 1 shows the illustration of the preparation process and the microscale structure of LNs/RGO.

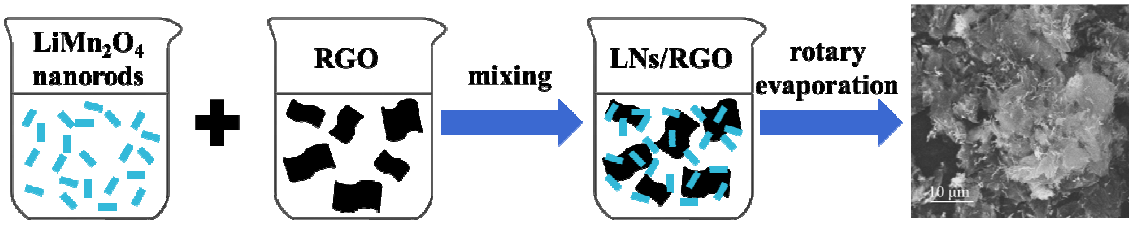

Fig. 1 Illustration of the preparation process and the microscale structure of LNs/RGO composite.

2.4 Characterization of the samples

The structure of the obtained samples was characterized by X-ray diffraction (XRD Rigaku D/MAX-r Adiffractometer) using Cu Kα radiation. Raman spectroscopy was carried out on a Renishaw (514 nm). The surface area analysis was conducted using Brunauer-Emmett-Teller (BET) theory (Quantachrome, nova 2000e). The morphology investigations were performed by scanning electron microscope (SEM，JSM-7000F, JEOL) with an energy dispersive X-ray spectrometer (EDS) and transmission electron microscope (TEM, Tecnai F20 at 200 kV).

2.5 Electrochemical measurements

Working electrodes were prepared by mixing 80 wt% active material (LNs, LNs/RGO or commercial LMO particles (LPs)), 10 wt% carbon black (Super-P), and 10 wt% PVDF in NMP solution to form homogenous slurry. After coating the above slurries on aluminum foil, the electrodes were dried at 120°C under vacuum for 24h to

remove the solvent. Electrode load was in the range of 3.4~3.6 mg/cm^2. Electrochemical experiments were performed using 2025 coin cells. The cells were assembled in an argon filled glove box with less than 0.5 ppm of oxygen and water, using lithium metal as the counter/reference electrode, a Celgard 2400 membrane as separator, and 1 M $LiPF_6$ electrolyte solution dissolved in a mixture of ethylene carbonate and dimethyl carbonate (v/v=1:1). Galvanostatic charge discharge cycles were tested by LAND electrochemical workstation at various C-rates between 3.1 to 4.3 V versus Li^+/Li at room temperature and at 55 ^oC, respectively. The electrochemical impedance spectroscopy (EIS) studies were carried out by applying a perturbation voltage of 5 mV in frequency range of 100 kHz to 0.01 Hz after 50 cycles at the fully discharged state, using CHI660D electrochemical workstation.

2. Results and discussion

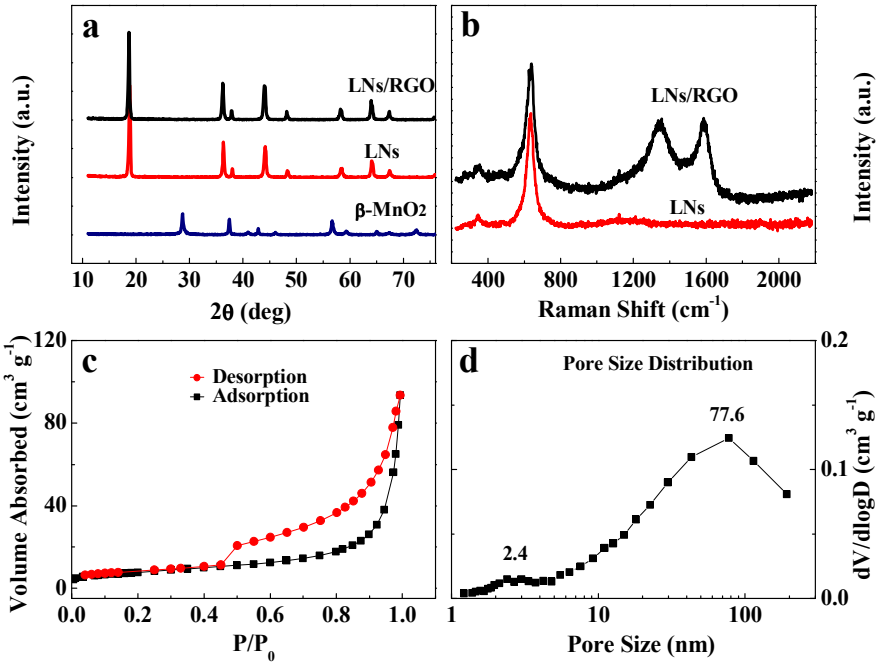

Fig. 2 (a) XRD patterns of LNs/RGO, LNs and β-MnO_2. (b) Raman spectra of LNs/RGO and LNs. (c) N_2 sorption isotherm and (d) pore size distribution of LNs/RGO.

Fig. 2a illustrates the XRD patterns of the β-MnO_2, LNs and LNs/RGO samples.

It can be seen that the MnO_2 powder obtained from the oxidation of manganese sulphate exhibits a pure ramsdellite phase with lower crystallinity (Fig.2a). The LNs XRD pattern showed features of the spinel structure with Fd3m space group (JCPS card No. 35-0782), with no peaks of the β-MnO_2 phase detected (Fig.2a). Additionally, the XRD pattern of the LNs/RGO shows that the (002) diffraction peaks of the graphene nanosheets cannot be detected, which may result from the low content of RGO in the hybrid.[17-20] Graphene nanosheets will be further characterized by Raman and transmission electron microcopy (TEM). Fig. 2b shows the Raman spectra of LNs and LNs/RGO. The intense peaks observed at 1351 and 1592 cm^{-1} in LNs/RGO are assigned to the D and G bands of graphene, respectively. The result proved that the LNs have been coated by graphene. Full nitrogen sorption isotherm of the LNs/RGO was measured to obtain the information on the pore size distribution and specific surface area. As shown in Fig. 2c, a type-IV isotherm with a type-H3 hysteresis loop in the relative pressure range of 0.45–1.0 P/P_0 indicates the presence of mesoporous structure. Accordingly, the specific surface area of LNs/RGO is calculated to be 27.5 m^2 g^{-1} via the Brunauer-Emmett-Teller (BET) method. The large BET surface area indicates that LNs/RGO has the large interface between the electrode material and the electrolyte. The pore size distribution derived from the BJH method is given in Fig. 2d. The bimodal pore size distribution was observed in LNs/RGO, which has two peaks corresponding macropores (77.6) nm and mesopores (2.4 nm). The abundant mesopores and macropores in the hybrid can serves as an “ion and electrolyte reservoir” to facilite the transportation of electrolyte ions, which is beneficial for the electrochemical performance of LNs/RGO.

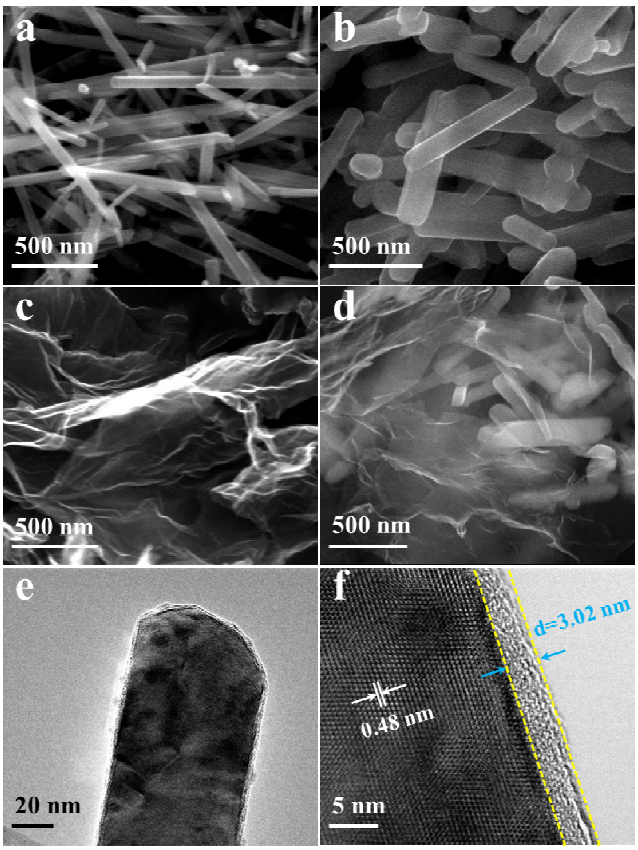

Fig. 3 SEM images of (a) β-MnO_2 nanorods, (b) LNs, (c) RGO and (d) LNs/RGO. The high-magnification (e) and high-resolution (f) TEM image of LNs/RGO.

Fig. 3 shows the SEM images of β-MnO_2, LNs and LNs/RGO. The SEM image (Fig. 3a) shows that the particles of β-MnO_2 consisted of nanorods with an average length of 2.5 μm. To confirm whether the nanorod morphology still maintained after the high temperature solid-state reaction, we performed SEM to analysis the morphology of LNs. Fig. 3b shows that the LNs phase still remained nanorods which appear to have a shorter average length of 1.2 μm than the as-prepared β-MnO_2. Fig. 3c shows the morphology characterization of pristine RGO nanosheets, which demonstrates its wrinkled paper-like structure. To make sure the introduction of RGO has homogenously distributed in the LNs, the SEM micrographs of the LNs/RGO are presented in Fig. 3d. The chemical composition and spatial distribution of LNs and RGO in the LNs/RGO are examined with EDS and elemental mapping analysis. As

shown in Fig. S1, the graphene nanosheets are uniformly distributed in the LNs/RGO composite samples. It suggests that the RGO can construct a highly conductive structure in the LNs/RGO and should influence the electrochemical performance.

The microstructure of the LNs/RGO was further investigated by TEM. As shown in Fig. 3e, LNs are homogeneously wrapped in the ultrathin graphene layers. Fig. 3f shows the HRTEM image taken from the edge of graphene wrapped LNs. The well-resolved lattice fringes with spacing of 0.48 nm correspond to the (111) planes of LNs, suggesting high-crystalline quality. The interlayer distance of graphene is approximately 0.38 nm and the wrapping layer has a thickness of about 3.02 nm which consists of eight monolayers of graphene. This further confirmed that the LNs are well wrapped in few-layer graphene nanosheets. The wrapped graphene nanosheets can not only effectively enhance the conductivity, but also can make the LNs/RGO more stable than pure LNs to against electrolyte etching.

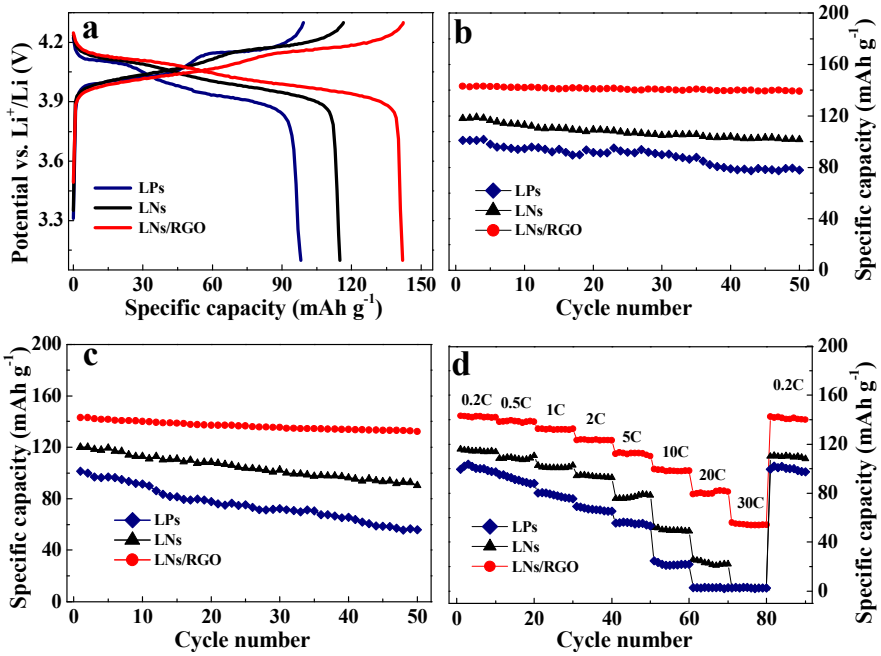

Fig. 4 Electrochemical performance of the LPs, LNs and LNs/RGO: (a) Charge and discharge curves, (b and c) cyclic performance at room temperature and 55 ^{o}C, respectively. (d) Rate performance of the LPs, LNs and LNs/RGO at the various C-rates.

In order to demonstrate the structural benefits of LNs/RGO for improving cathode performance, a series of electrochemical measurements were carried out. Commercial LMO particles (LPs) were purchased as control sample. Representative charge-discharge curves of the LPs, LNs and LNs/RGO at the rate of 0.2 C are shown in Fig 4a. There are two pseudoplateaus at around 3.9 and 4.1 V in the charge and discharge curves which are the typical electrochemical behavior of spinel LMO.[16] LPs and LNs show a coulombic efficiency of 98%. After introduced RGO, the LNs/RGO exhibits excellent performance with a coulombic efficiency of nearly 100%. The good performance of LNs can be easily observed in Fig 4a. The capacity of LNs approaches to 118.9 mAh g^{-1}, which is higher than that of the LPs (100.9 mAh g^{-1}). Compared to the LPs, LNs not only have large surface areas and short diffusion lengths but also provides efficient electron transport pathways,[16] which results in the good electrochemical performance of LNs.

The LNs/RGO shows excellent electrochemical performance with high capacity of 143.5 mAh g^{-1} as shown in Fig. 4b. After 50 cycles, the LNs/RGO exhibits excellent cyclic performance with a capacity retention of ~97%, which is better than that of LNs (~85%). The graphene sheets with high conductivity in LNs/RGO serve as the conductive channels between LNs, which leads to the high specific capacity. The LNs/RGO also exhibits good cycling stability at elevated temperature (up to 50 ^{o}C) as shown in Fig. 4c. The capacity retention increases from 75.3% to 90.4%. It indicates that the wrapped RGO can make the LNs/RGO more stable than pure LNs to against electrolyte etching during cycling at elevated temperature.

The rate performances of the three samples have been shown in Fig. 4d. When C-rate increases to 0.5,1, 3, 5, 10, 20, and 30 C, respectively, discharge capacity of the LNs/RGO cathode decreases to139.5, 132.6, 123.8, 112.6, 99.5, 82.1, and 56 mAh g^{-1}, respectively. Remarkably, the capacities at 10 C (1.48 A g^{-1}) and 20 C (2.96 A g^{-1}) are still 99.5 and 82.1 mAh g^{-1}, respectively; at 30 C (4.44 A g^{-1}) it drops to 56 mAh g^{-1}. Moreover, the capacity can be well recovered (141.6 mAh g^{-1}) when the C-rate is changed from 4C to 0.1C, showing the high reversibility of the system. The excellent

rate performance can be attributed to the synergetic effect of the LNs matrix and the conductive graphene wrapping layers. On the one hand, the graphene in LNs/RGO can effectively enhance the conductivity of composite; on the other hand, the large specific area with massive mesopores and macropores can greatly enhance the electrolyte/electrode contact. In addition, the nanostructure with ultrathin graphene wrapped LMO nanorods can effectively reduce the diffusion length of both electrons and ions.

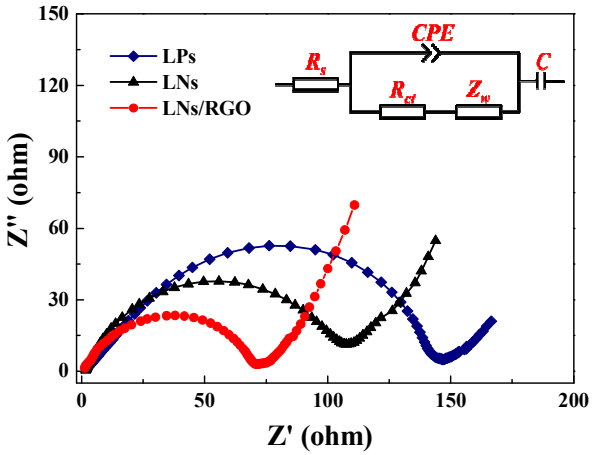

Fig. 5 Nyquist plots of LPs, LNs and LNs/RGO after 50 cycles.

In order to confirm the structural stability of LNs/RGO, the post-mortem SEM analysis was performed on the electrodes after 50 cycles. As shown in Fig. S2, no mechanical crack can be found on the surface of the electrode, verifying the robust properties of LNs/RGO. To further understand the effects of graphene sheets in the LNs, the electrochemical impedance spectroscopy (EIS) has been performed. Fig. 6 shows the EIS spectra of LPs, LNs and LNs/RGO after 50 cycles. For all of these cells, the spectra of those three electrodes consist of a semicircle at high-middle frequencies attributed to the charge-transfer reaction and an oblique linear Warburg part at low frequencies attributed to the Li ion diffusion.[21] After simulating the data by the software of ZView, the exactly mount of the resistance was displayed in Table 1. Here R_s and R_{ct} represent the solution resistance and charge transfer resistance at the particle/electrolyte interface. It can be observed that R_s of the graphene modified LNs

are similar to the pure LNs whereas the LNs/RGO has much smaller charge transfer resistance than that of LNs. Therefore, the smaller charge transfer resistance of the modified electrodes further proves that the introduced graphene can improve electrical conductivity of the LNs.

Table 1

The impedance parameters of the LPs, LNs and LNs/RGO electrodes.

Materials	R_s (Ω)	R_{ct} (Ω)
LPs	2.7	147.5
LNs	2.6	119.3
LNs/RGO	1.1	70.4

The significant performance enhanced by graphene nanosheets can be simply interpreted as the synergetic effect of $LiMn_2O_4$ nanorods matrix and conductive graphene wrapping layers. On the one hand, Li-ion diffusion strongly depends on the transport length and accessible sites on the surface of active materials.[16, 22, 23] Therefore, nanostructured electrodes of LNs/RGO offer higher capacity and better cycling stability due to the large electrode/electrolyte contact area, short path length for Li ion transport, and good stability; on the other hand, due to the high conductivity of the wrapped graphene layer, the electrons can be fast transferred on the surface of LNs; in addition, due to the large specific surface area of graphene, it could provide more paths for the Li ion pass which is favorable for Li ion migration between the cathode and electrolyte. Based on the synergetic effect mentioned above, RGO wrapped LNs cathode exhibits smaller impedance, better cycling stability, much higher specific capacity, and much better high-rate performance.

4. Conclusions

In summary, we present a facile eco-Friendly method with ethanol assisted dispersion combined with magnetic stirrer to prepare reduced graphene oxide (RGO) wrapped $LiMn_2O_4$ nanorods (LNs). LNs/RGO can effectively utilize the good

conductivity and high surface area of graphene, as well as the large electrode/electrolyte contact area and short path length for Li ion transport of LNs. As a result, the LNs/RGO exhibits high reversible capacity (143.5 $mAhg^{-1}$), excellent cyclic performance (97% capacity retention), and good rate capability (56 mAh g^{-1} at 30 C). The synergetic effect of the $LiMn_2O_4$ nanorods matrix and the conductive graphene wrapping layers might lead to the significant performance enhancement. The excellent electrochemical properties make LNs/RGO as promising cathode material for high-performance LIBs. In addition, the facile synthesis routine enables the mass production and can be extended to prepare other graphene wrapped anode or cathode electrodes for LIBs.

Acknowledgments

The research was supported by the National Natural Science Foundation of China (Grant Nos. 51372033, 51202022, and 61378028), the National High Technology Research and Development Program of China (Grant no. 2015AA034202), the 111 Project (Grant No. B13042), the Specialized Research Fund for the Doctoral Program of Higher Education (Gran No. 20120185120011), Sichuan Youth Science and Technology Innovation Research Team Funding (Grant No. 2011JTD0006), the Fundamental Research Funds for the Central Universities (Grant No. ZYGX2013Z001), and the Sino-German Cooperation PPP Program of China.

References:

1 B. Kang, G. Ceder, *Nature*, 2009**,** ***458*****,** 190-193.
2 J. M. Tarascon, M. Armand, *Nature*, 2001**,** ***414*****,** 359-367.
3 M. Armand, J. M. Tarascon, *Nature*, 2008**,** ***451*****,** 652-657.
4 F. Cheng, H. Wang, Z. Zhu, Y. Wang, T. Zhang, Z. Tao, J. Chen, *Energ Environ Sci*, 2011**,** ***4*****,** 3668.
5 W. Tang, Y. Hou, F. Wang, L. Liu, Y. Wu, K. Zhu, *Nano Lett*, 2013**,** ***13*****,** 2036-2040.
6 Y. Wang, G. Cao, *Adv Mater*, 2008**,** ***20*****,** 2251-2269.
7 Y. Guo, J. Hu, L. Wan, *Adv Mater*, 2008**,** ***20*****,** 2878-2887.
8 B. Zou, X. Ma, Z. Tang, C. Ding, Z. Wen, C. Chen, *J Power Sources*, 2014**,** ***268*****,**

491-497.
9 H. Xia, K. R. Ragavendran, J. Xie, L. Lu, *J Power Sources*, 2012**,** ***212*****,** 28-34.
10 W. Tang, X. J. Wang, Y. Y. Hou, L. L. Li, H. Sun, Y. S. Zhu, Y. Bai, Y. P. Wu, K. Zhu, T. van Ree, *J Power Sources*, 2012**,** ***198*****,** 308-311.
11 X. Zhou, F. Wang, Y. Zhu, Z. Liu, *Journal of Materials Chemistry*, 2011**,** ***21*****,** 3353.
12 J. He, Y. Chen, P. Li, Z. Wang, F. Qi, J. Liu, *Rsc Adv*, 2013**,** ***4*****,** 2568.
13 Y. Ding, H. Ren, Y. Huang, F. Chang, X. He, J. Fen, P. Zhang, *Nanotechnology*, 2013**,** ***24*****,** 375401.
14 Y. Ding, Y. Jiang, F. Xu, J. Yin, H. Ren, Q. Zhuo, Z. Long, P. Zhang, *Electrochem Commun*, 2010**,** ***12*****,** 10-13.
15 D. Li, M. B. Muller, S. Gilje, R. B. Kaner, G. G. Wallace, *Nat Nanotechnol*, 2008**,** ***3*****,** 101-105.
16 D. K. Kim, P. Muralidharan, H. Lee, R. Ruffo, Y. Yang, C. K. Chan, H. Peng, R. A. Huggins, Y. Cui, *Nano Lett*, 2008**,** ***8*****,** 3948-3952.
17 Q. Zhang, W. Peng, Z. Wang, X. Li, X. Xiong, H. Guo, Z. Wang, F. Wu, *Solid State Ionics*, 2013**,** ***236*****,** 30-36.
18 P. Lian, X. Zhu, S. Liang, Z. Li, W. Yang, H. Wang, *Electrochim Acta*, 2011**,** ***56*****,** 4532-4539.
19 Q. Wang, L. Jiao, H. Du, Y. Wang, H. Yuan, *J Power Sources*, 2014**,** ***245*****,** 101-106.
20 M. Zhou, T. Cai, F. Pu, H. Chen, Z. Wang, H. Zhang, S. Guan, *Acs Appl Mater Inter*, 2013**,** ***5*****,** 3449-3455.
21 Z. S. Wu, W. Ren, L. Xu, F. Li, H. M. Cheng, *Acs Nano*, 2011**,** ***5*****,** 5463-5471.
22 C. Peng, B. Chen, Y. Qin, S. Yang, C. Li, Y. Zuo, S. Liu, J. Yang, *Acs Nano*, 2012**,** ***6*****,** 1074-1081.
23 M. Okubo, Y. Mizuno, H. Yamada, J. Kim, E. Hosono, H. Zhou, T. Kudo, I. Honma, *Acs Nano*, 2010**,** ***4*****,** 741-752.